ACS APPLIED MATERIALS & INTERFACES

Research Article

www.acsami.org

Gradient Mechanical Properties Facilitate *Arabidopsis* Trichome as Mechanosensor

Han Liu,[†,‡] Li Hong Zhou,[§] Jiaojiao Jiao,[‡,∥] Shaobao Liu,[‡,∥] Zhanming Zhang,[⊥] Tian Jian Lu,[‡,∥] and Feng Xu*[,†,‡]

[†]The Key Laboratory of Biomedical Information Engineering of Ministry of Education, School of Life Science and Technology, Xi'an Jiaotong University, Xi'an 710049, P. R. China

[‡]Bioinspired Engineering and Biomechanics Center (BEBC), Xi'an Jiaotong University, Xi'an 710049, P. R. China

[§]College of Life Sciences, Agricultural University of Hebei, Baoding 071001, P. R. China

[∥]State Key Laboratory for Mechanical Structure Strength and Vibration, Xi'an Jiaotong University, Xi'an 710049, P. R. China

[⊥]State Key Laboratory for Mechanical Behavior of Materials, Xi'an Jiaotong University, Xi'an 710049, P. R. China

Supporting Information

ABSTRACT: It has been reported that *Arabidopsis thaliana* leaf trichome can act as a mechanosensory switch, transducing mechanical stimuli into physiological signals, mainly through a buckling instability to focus external force (e.g., exerted by insects) on the base of trichome. The material and structural properties of trichomes remain largely unknown in this buckling instability. In this report, we mainly focused on material standpoint to explore the possible mechanism facilitating the buckling instability. We observed that the Young's modulus of trichome cell wall decreased gradually from branch to the base region of trichome. Interestingly, we also found a corresponding decline of calcium concentration on the trichome cell wall. Results of finite element method (FEM) simulation suggested that such a gradient distribution of Young's modulus significantly promotes force focusing and buckling instability on the base of trichome. It is indicated that *Arabidopsis* trichome has developed into an active mechanosensor benefiting from gradient cell wall mechanical properties.

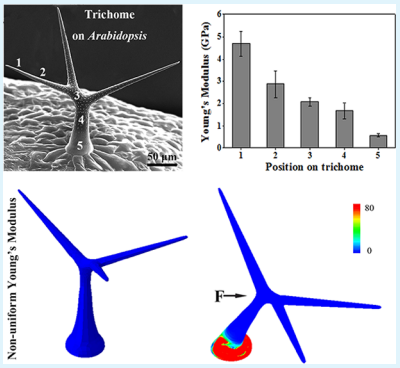

KEYWORDS: *Arabidopsis trichome, mechanosensor, Young's modulus, calcium concentration, papillae*

1. INTRODUCTION

In the long period of evolution, plants have dynamically evolved with different epidermis and derived structures,[1,2] such as trichomes, spines, and toughened leaves, to defend themselves against various biotic and abiotic stresses (e.g., fungi, bacteria, drought, and torridity). Among these specialized structures, trichome has attracted special interest because tremendous species-specific diversity enables the trichome to have a variety of functions,[3,4] such as creating a microshell of relatively high humidity to reduce water transpiration, reflecting light to protect plants against UV radiation, and forming a mechanical barrier to prevent insect attack.[5−7] Such functions are closely related to the structural traits and material properties of the trichome, such as element concentration and mechanical characteristics. Nevertheless, most existing studies on trichomes have focused on trichome morphogenesis and their defensive role mainly from the perspective of physiology or biochemical molecular fields.[8−10] The structural characteristics and material properties of trichome are still poorly understood.

Arabidopsis trichome has been widely used as a model system for studying the biological behaviors of plant cells, including the molecular mechanisms of differentiation and pattern formation.[11,12] Trichomes on *Arabidopsis*, originating from epidermal cells, are nonglandular and unicellular hairs with bulged base and three to five branches exhibiting an unusual antenna-like morphology,[13−16] and mature leaf trichomes are about 200−500 μm tall and 40−60 μm wide at the trichome base.[17,18] As a special structure of *Arabidopsis* leaves, trichomes have been found to form a mechanical barrier to prevent insect attack.[19,20] Specifically, when insects alight and move on a leaf, they will mechanically stimulate the trichome, which might vibrate slightly under weak disturbance or elicit a buckling instability on its base under strong compression.[21−23] It has also been reported that trichomes on *Cucurbita* leaves are associated with collenchyma in petioles to affect the potential reorientation of the leaf and maintain the prestressed state of petioles. In other words, trichomes on *Cucurbita* can act as a biomechanical structure.[24] It was interestingly noted that, in order to prevent microbial infection and herbivores, *Arabidopsis* leaves could produce a variety of secondary metabolites that contain a group of glucosinolate, alongside protease inhibitors, terpenoid volatiles, and phenolic species.[25−28] In addition, our group has previously observed that the trichome can act as an active mechanosensory switch. When mechanically stimulated,

Received: February 23, 2016
Accepted: March 24, 2016
Published: March 24, 2016

DOI: 10.1021/acsami.6b02253
ACS Appl. Mater. Interfaces 2016, 8, 9755−9761

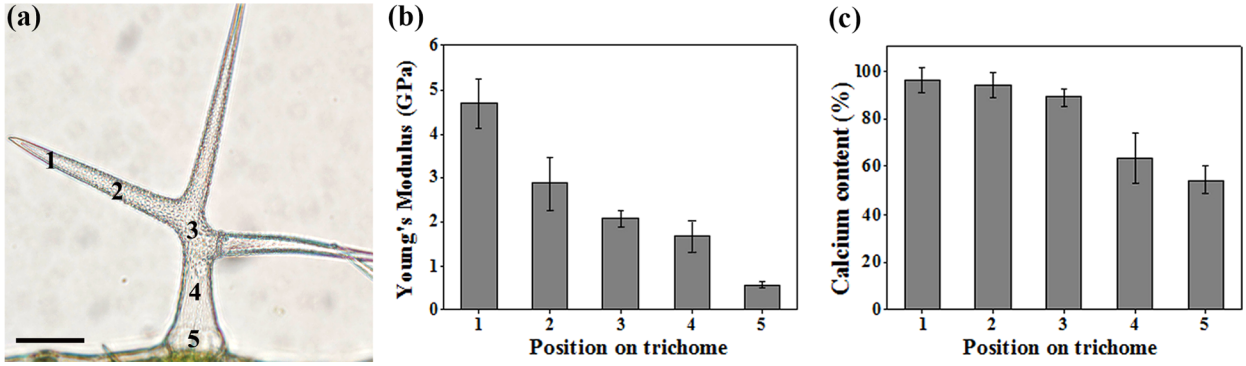

Figure 1. Young's modulus of trichome changed gradually from branch to stalk and base. (a) Microstructure of the trichome from one-month-old wild-type *Arabidopsis* imaged by inverted phase contrast microscope. The numbers 1−5 indicate five different regions on trichome. Scale bar = 50 μm. (b) Young's modulus of trichome different regions. (c) Using potassium as internal standard, energy dispersive spectroscopy was used to quantitatively detect calcium concentration at different regions of trichome. Error bars in parts b and c represent standard deviations.

trichome can focus force on the base region leading to a buckling deformation or instability. Such buckling instability can elicit Ca^{2+} oscillations and pH shifts in surrounding cells, transducing mechanical signals to epidermal cells.[23] Additionally, consistent with Kulich et al.,[29] our group also found that the thickness of trichome cell wall was nonuniform, which can facilitate the buckling instability on trichome base.[23] However, other factors contributing to the buckling instability, especially trichome cell wall material properties, are yet to be considered.

From the structure standpoint, the nonuniform thickness cell wall of trichome can make it easier to focus the force to its stalk base and hence induce buckling instability.[29] However, from the material standpoint, much less attention was paid to exploring mechanical properties of trichome cell wall which might facilitate buckling instability. Considering the nonuniform cell wall thickness, it is reasonable to assume that the Young's modulus of the trichome cell wall could be nonuniform as well. In this report, we mainly focused on trichome cell wall material properties to explore further physical mechanism of buckling instability on the trichome base.

2. EXPERIMENTAL SECTION

2.1. Plant Materials and Growth Conditions. *Arabidopsis* ecotype Columbia was used in this study. Plants were grown in a Turba substrate (Kekkila DSM 2W) from Kekkila Garden (Vantaa, Finland) in a growth chamber with an average photon flux density of 90−120 μmol m^{-2} s^{-1} at 22 °C; the light cycle is 16 h of light (7 a.m. to 11 p.m.) and 8 h of darkness (11 p.m. to 7 a.m.). Before seeds were sown in soil, they were pretreated at 4 °C for 3 days.

2.2. SEM and Elemental Analysis by SEM−EDS. One-month-old *Arabidopsis* leaves were freeze-dried and mounted on a double-sided carbon tape and were then sputtered with a thin layer of gold. To avoid the influence of plant age and the different degree of maturation, we analyzed trichomes on the fourth leaves of a one-month-old plant. The microstructure of trichome was scanned under a focused beam of high energy electrons in raster scan pattern, and the scanning electron microscopy (SEM) analysis was carried out in a high vacuum mode using an ultrahigh resolution field emission scanning electron microscope ZEISS MERLIN Compact with 10 keV of operating power source. Element analysis of trichomes' cell walls was performed through energy dispersive X-ray spectroscopy (EDS) with EDAX Apollo XP detector operating at an accelerating voltage of 10 keV at high vacuum mode. Mapping analysis of element concentration and distribution was conducted through energy dispersive X-ray spectroscopy (EDS) as well. Elemental concentration obtained from EDS was calculated as weight percentage (%).

2.3. Nanoindentation. The mechanical properties of the trichome were measured using a Hysitron TI950 TriboIndenter (Hysitron). The indentations were performed using a Berkovich indentor. More details about nanoindentation were described in Supporting Information. To minimize the influence that may be induced by the hollow structure of trichome branch and stalk, we employed force control mode and tested different forces from 100 to 1000 μN. Considering the minimization of deformation impact on trichome, finally, we set 200 μN to measure the Young's modulus of trichome.

2.4. Finite Element Method (FEM) Simulation. On the basis of SEM images of a trichome, a three-dimensional geometry model of trichome was developed by using a standard computer-aided design software (Creo, PTC, Needham, MA). The overall dimensions of trichomes were obtained from the SEM image of a mature tirchome, where cell wall thickness was assigned as 1.5−6 μm as studied by Zhou et al.[23,29] The cell wall was thickened ranging from the tip of the branch to the connection region. In the model, the cell wall thickness of the connection region was set as 6 μm. Due to the thickness tapering rapidly from the stalk to the base of the trichome, accordingly the thickness of the base region was assigned as 1.5 μm. Then, the geometry data were imported into a finite element analysis software (ABAQUS 6.13) where the cell wall of trichome was modeled as a shell with nonuniform thickness and Young's modulus. The value of the uniform Young's modulus was assigned as 2.3 GPa, while nonuniform Young's modulus was assigned as 0.6−2.3 GPa from trichome base to the connection region and 2.3−5.0 GPa from the connection region to the branch tip according to the measurement result with linear interpolation. The trichome was meshed with S4R and S3 shell elements, and the element shape was quad-dominated (mesh size 4 μm). The buckling behavior was simulated both at normal and shear force. The strain energy density (SED) was nondimensionalized by the mean strain energy density (MSED). Herein, MSED was calculated by MSED = $\int_V \sigma \, d\varepsilon/V = \int_l F_R \, dl/V$, where F_R is the reaction force, l is the displacement at the loading points, and V is the volume of trichome cell wall.

3. RESULTS AND DISCUSSION

To test the Young's modulus of the trichome cell wall, we performed nanoindentation experiments at different regions (i.e., branch, connection domain, stalk and base) of mature trichome as shown in Figure 1a, which was isolated from the fourth leaves of a one-month-old plant. The gradient image of indentations on the pressed trichome branch was shown in Figure S2. We found that the Young's modulus decreased gradually from branch tip (region 1), to connection region (region 3) and base (region 5) as shown in Figure 1b. For instance, the Young's modulus at branch tip was 4.698 ± 0.54 GPa, nearly 10 times higher than that at stalk base (0.577 ±

DOI: 10.1021/acsami.6b02253
ACS Appl. Mater. Interfaces 2016, 8, 9755−9761

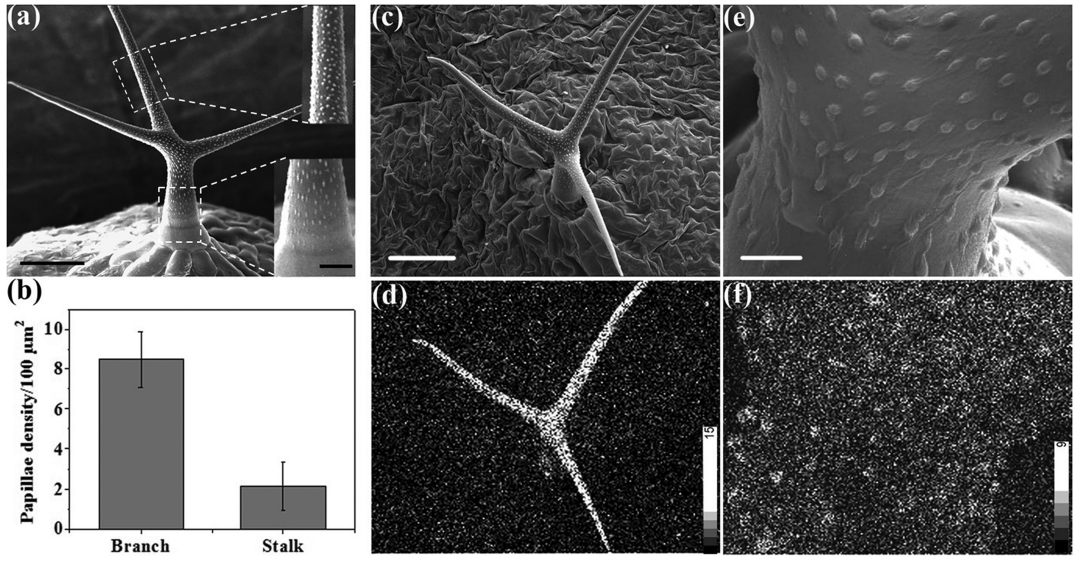

Figure 2. Gradient of calcium concentration positively correlated with papillae density. (a) Scanning electron micrograph of a mature trichome, where higher magnification images of branch and stalk are included as the inset. Scale bar for the whole trichome is 50 μm. Scale bar for insert is 10 μm. (b) Papillae density determined as the number of papillae per 100 μm^2. (c) Scanning electron micrograph of a mature trichome, scale bar is 60 μm. (d) Map analysis of calcium concentration on trichome. (e) Higher magnification of trichome connection region, scale bar is 10 μm. (f) Map analysis of calcium concentration on the connection region of three branches of trichome. Error bars in part b represent standard deviations.

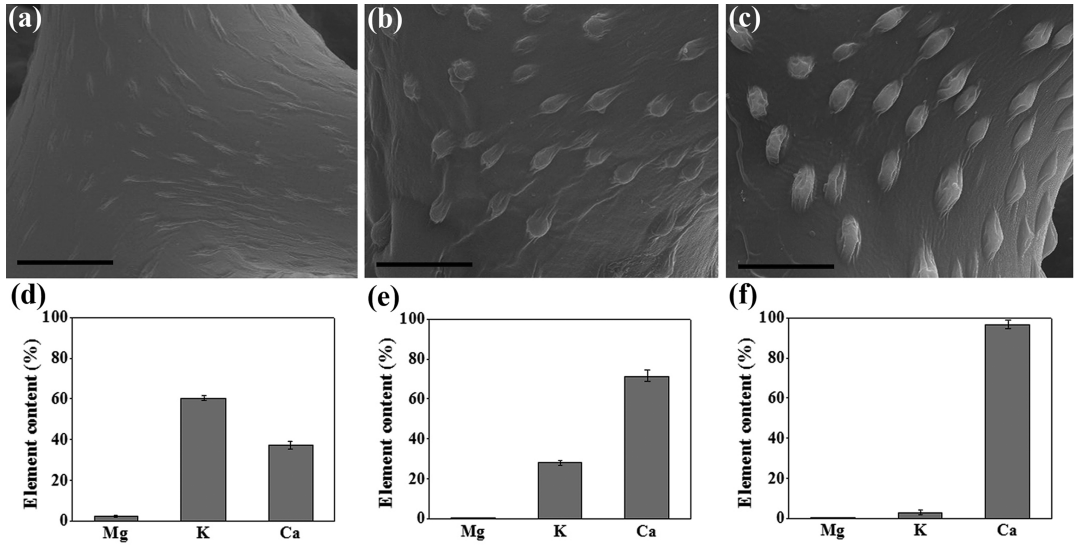

Figure 3. Calcium on trichome cell wall increased with papillae development. (a–c) SEM images of papillae at different growth stage, from part a to part c means from young to mature. Scale bar is 10 μm. (d–f) Using Mg, K as internal standards, energy dispersive spectroscopy was used to qualitatively detect calcium concentration in trichomes with three different growth stages. (d) Calcium concentration in part a. (e) Calcium concentration in part b. (f) Calcium concentration in part c. Error bars in parts d–f represent standard deviations.

0.06 GPa). These findings indicate that the nonuniform spatial distribution of cell wall material property from the branch to the base might make it easier for trichome to serve as a mechanical transducer. It should be noted that the native leaf is wavy, which is not suitable for testing in the sample chamber. Additionally, isolated trichomes need to be freeze-dried and pasted on a hard substrate since nanoindentation could not be performed on wet and unfixed samples. Furthermore, water in trichome mainly exists in the central vacuole; the freeze-drying step used in nanoindentation was speculated to have no significant influence on cell wall structures and material properties. Besides, all samples were treated in the same way; therefore, the mechanical properties of trichome wall can be compared at a relative basis.[30]

It has been well-known that pectin as an important composition is abundant in the trichome cell wall,[31] while calcium ions, as a vital factor in normal plant growth, are prone to bind with pectin to form calcium pectate, crucial for stabilization of cell wall structures.[32,33] Thus, it is conceivable that calcium on the trichome cell wall might be abundant as well. Therefore, inspired from the Young's modulus results, we examined calcium concentration and its spatial distribution on trichome cell wall by performing SEM–EDS at the same five regions of trichome (Figure 1c). Elemental analysis revealed that the calcium concentration also decreased gradually from

DOI: 10.1021/acsami.6b02253
ACS Appl. Mater. Interfaces 2016, 8, 9755–9761

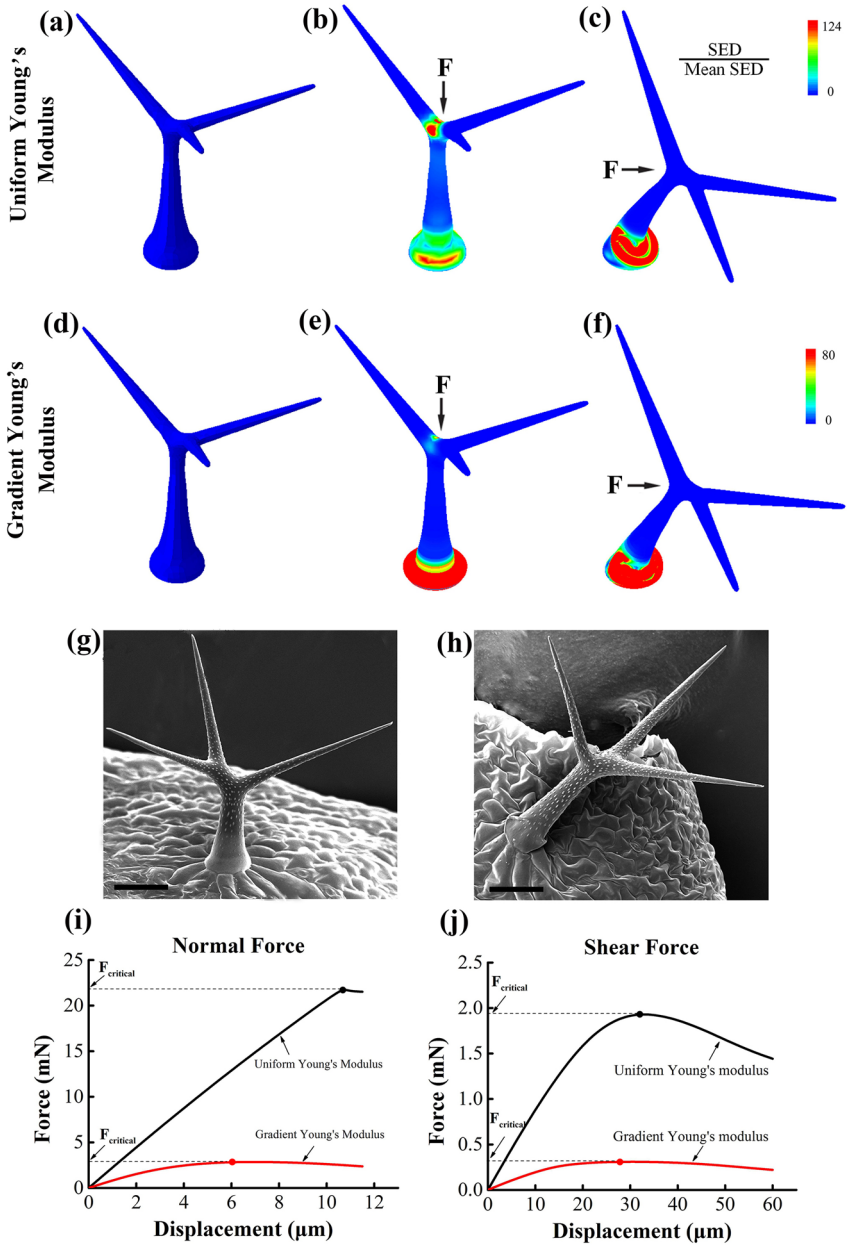

Figure 4. FEM simulation and experiments of trichome buckling inability. (a–c) Control group: trichomes with nonuniform cell wall thickness but with uniform Young's modulus at the loads of normal force and shear force. (d–f) Test group: trichomes with nonuniform cell wall thickness and with nonuniform Young's modulus at the loads of normal force and shear force. The color in (a–f) represents the dimensionless strain energy density. (g, h) Scanning electron micrograph of trichome under normal condition (g) and compression by a moderate force (h). Scale bar = 50 μm. (i, j) The relationship of reaction force and displacement at the loading points under the loads of normal force and shear force. Dots on lines mean the critical points.

branch tip to the base region, consistent with the variation of cell wall modulus. It should be noted that SEM analysis requires dry tissue, which may not be the same as the fully hydrated leaves *in vivo*. The freeze-drying step used to prepare the samples for SEM–EDS has been shown to have no significant influence on cell wall structures and material properties.[34−36] We also observed no significant change of the trichome structure after processing.

To further explore the mechanism of calcium distribution on the trichome, our focus was next placed upon the protrusion on the trichome surface (i.e., papillae), since papillae act as subcuticular depositions of the trichome cell wall.[7,37−39] We visually observed that the density papillae on trichome branch was higher than that on the stalk (Figure 2a). We then quantified the papillae density and found, on average, 8.5 ± 1.4 papillae per 100 μm^2 trichome area on the branch, which was about 4 times higher than that on stalk (2.1 ± 1.2) (Figure 2b). On the basis of these findings, we speculated a positive correlation between calcium concentration and papillae density on trichome surface. For validation, we performed SEM-EDS mapping analysis to image the distribution of individual element, e.g., carbon, oxygen, potassium, and calcium. Corresponding results shown in Figure 2c–f indicated that calcium was richer on papillae compared with that in the nonpapillae region, thus confirming the positive correlation between calcium concentration and papillae density. Built upon

DOI: 10.1021/acsami.6b02253
ACS Appl. Mater. Interfaces 2016, 8, 9755–9761

this, we assumed that papillae might possess the ability to gather calcium. To examine this, we performed SEM−EDS analysis of trichomes with different growing stages (Figure 3a−c) and observed a gradual increase of calcium concentration with increasing papillae size (Figure 3d−f). To further verify the calcium collecting ability of papillae, we examined the first true leaf of a 7-day-old *Arabidopsis* and found that young trichomes with no papillae have less calcium concentration compared with older ones with high papillae density (Figure S3). Taken together, these data indicate that papillae have the ability to collect calcium and thus enrich the calcium concentration of trichome, which might affect the mechanical properties of the trichome cell wall, such as the Young's modulus. Additionally, Suo et al. have reported that mutants of *GLASSY HAIR (GLH)* genes showed phenotypes with reduced papillae formation and significant reduction of cellulose content,[7] indicating that a positive correlation might exist between papillae density and cell wall mechanical properties. Trichome of the *EXO70H4-1* gene mutant, as reported by Kulich et al., was covered with papillae but failed on development of the secondary cell wall of trichome.[29] Thus, we should pay more attention to mutants to investigate the material properties and functions about papillae in the furture.

To examine whether the gradient distribution of Young's modulus on the trichome cell wall could promote buckling and force focusing in the stalk base, we analyzed the mechanical response of typical trichomes by FEM simulation (Figure 4). Since external loading on the trichome is stored as strain energy, we first compared the strain energy density of a trichome having uniform Young's modulus (Figure 4a−c) to that with gradient Young's modulus (Figure 4d−f). To facilitate the FEM simulation, external forces exerted on a trichome from nature (e.g., by insects) could be equivalent to normal forces (Figure 4b,e) and shear forces (Figure 4c,f) acting on the connection part of three branches on the trichome. Under normal compression, for the case of uniform Young's modulus, the greatest density of strain energy was found not only on the base of trichome, but also on the connection part (red region) (Figure 4b). In contrast, for the case of gradient Young's modulus, the greatest density of strain energy was only found on the trichome base (Figure 4e). Under shear force, however, the strain energy density was mainly focused on the trichome base (Figure 4c,f), whether the Young's modulus is uniform or not. While the simulation results agree in general with experimental observations (Figure 4g,h), negligible variance in buckling instability was found (Figure 4h) owing to the difficulty in experiments of precisely controlling the compression on trichome. To quantitatively characterize the buckling behavior of trichome, we analyzed the relationship between reaction force and displacement at the loading point for both normal (Figure 4i) and shear (Figure 4j) forces. In either case, we found that there exists a critical point of the buckling force. More importantly, the critical force for the case of gradient modulus is significantly smaller than the uniform case, indicating that it is much easier for a trichome with gradient Young's modulus to initiate buckling instability and thus efficiently sense or transduce mechanical signals. Specifically, in response to the shear force, the critical load of buckling was about 2 mN for a trichome with uniform modulus, about 10 times greater than that with gradient modulus (0.3 mN) (Figure 4h). With 2 mN buckling force for a trichome with uniform modulus, only larger herbivores such as feeding cabbage loopers (20−40 mN) or mirid bugs (2−6 mN) might effectively perturb the trichome.[40,41] In sharp contrast, a much smaller shear force (0.3 mN) could induce buckling instability in a trichome with gradient Young's modulus, implying that trichomes on *Arabidopsis* leaves are very sensitive: even small insects such as aphid might have the ability to disturb *Arabidopsis* trichomes effectively.[42,43] Since bending stiffness (EI) is strongly dependent on cell wall geometry, we also calculated bending stiffness of base, stalk, and connection, which are 2.96×10^{-11}, 3.71×10^{-11}, 7.88×10^{-11} N m^2, respectively. The deformation of trichome under the shear force includes the bending deformation and buckling deformation. Such gradient of bending stiffness may make it easier to reach critical load and cause buckling on the trichome base, which is critical for mechanical signal transduction.

4. CONCLUSIONS

In this report, we found that the Young's modulus of the trichome cell wall decreased gradually from branch tip to connection region and base, correlating well with the gradual decrease of calcium concentration. We also found papillae, which covered on the surface of trichome cell wall, owned the ability to collect calcium. FEM simulations further showed that gradient Young's modulus can significantly reduce the critical force of buckling instability on trichome base, and enhance the sensitivity of trichome which acts as a mechanosensor. These findings suggest that nonuniform spatial distribution of cell wall mechanical properties from connection region to the base make it easier for trichome to serve as mechanosensor, which inspire us to study more about biomimetic engineering in the future. Moreover, it seems quite necessary to extend our research to other plants, especially crops.

■ ASSOCIATED CONTENT

Supporting Information

The Supporting Information is available free of charge on the ACS Publications website at DOI: 10.1021/acsami.6b02253.

Nanoindentation description and additional figures showing schematic representation of load versus indenter displacement, scan image of trichome branch pressed by a nanoindentor, and calcium concentration on trichomes (PDF)

■ AUTHOR INFORMATION

Corresponding Author

*E-mail: fengxu@mail.xjtu.edu.cn.

Author Contributions

H.L., L.H.Z., and Z.Z. performed experimental work and data analysis. J.J. and S.L. performed theoretical work. F.X. and T.J.L. planned the project. All authors wrote and revised the paper.

Notes

The authors declare no competing financial interest.

■ ACKNOWLEDGMENTS

This work was financially supported by the National Natural Science Foundation of China (11372243, 11522219,11532009) and the Key Program for International S&T Cooperation Projects of Shaanxi. We thank Prof. Guy Genin and Prof. Barbara Pickard for the helpful discussions. All the work was performed at Bioinspired Engineering and Biomechanics Center.

DOI: 10.1021/acsami.6b02253
ACS Appl. Mater. Interfaces 2016, 8, 9755−9761

REFERENCES

(1) Bednarek, P.; Osbourn, A. Plant-Microbe Interactions: Chemical Diversity in Plant Defense. *Science* **2009**, *324*, 746−748.
(2) Remans, R.; Spaepen, S.; Vanderleyden, J. Auxin Signaling in Plant Defense. *Science* **2006**, *313*, 171−171.
(3) Hulskamp, M. Plant Trichomes: A Model for Cell Differentiation. *Nat. Rev. Mol. Cell Biol.* **2004**, *5*, 471−480.
(4) Bernhardsson, C.; Robinson, K. M.; Abreu, I. N.; Jansson, S.; Albrectsen, B. R.; Ingvarsson, P. K. Geographic Structure in Metabolome and Herbivore Community Co-Occurs with Genetic Structure in Plant Defence Genes. *Ecol. Lett.* **2013**, *16*, 791−798.
(5) Nayidu, N. K.; Tan, Y. F.; Taheri, A.; Li, X.; Bjorndahl, T. C.; Nowak, J.; Wishart, D. S.; Hegedus, D.; Gruber, M. Y. Brassica Villosa, a System for Studying Non-Glandular Trichomes and Genes in the Brassicas. *Plant Mol. Biol.* **2014**, *85*, 519−539.
(6) Hanley, M. E.; Lamont, B. B.; Fairbanks, M. M.; Rafferty, C. M. Plant Structural Traits and Their Role in Anti-Herbivore Defence. *Perspect. Plant Ecol. Evol. Syst.* **2007**, *8*, 157−178.
(7) Suo, B. X.; Seifert, S.; Kirik, V. Arabidopsis Glassy Hair Genes Promote Trichome Papillae Development. *J. Exp. Bot.* **2013**, *64*, 4981−4991.
(8) Schilmiller, A. L.; Last, R. L.; Pichersky, E. Harnessing Plant Trichome Biochemistry for the Production of Useful Compounds. *Plant J.* **2008**, *54*, 702−711.
(9) Tian, D. L.; Tooker, J.; Peiffer, M.; Chung, S. H.; Felton, G. W. Role of Trichomes in Defense against Herbivores: Comparison of Herbivore Response to Woolly and Hairless Trichome Mutants in Tomato (Solanum Lycopersicum). *Planta* **2012**, *236*, 1053−1066.
(10) Holeski, L. M.; Chase-Alone, R.; Kelly, J. K. The Genetics of Phenotypic Plasticity in Plant Defense: Trichome Production in Mimulus Guttatus. *Am. Nat.* **2010**, *175*, 391−400.
(11) Balkunde, R.; Pesch, M.; Hulskamp, M. Trichome Patterning in Arabidopsis Thaliana from Genetic to Molecular Models. *Curr. Top. Dev. Biol.* **2010**, *91*, 299−321.
(12) Pattanaik, S.; Patra, B.; Singh, S. K.; Yuan, L. An Overview of the Gene Regulatory Network Controlling Trichome Development in the Model Plant, Arabidopsis. *Front. Plant Sci.* **2014**, *5*, 259.
(13) Mathur, J.; Chua, N. H. Microtubule Stabilization Leads to Growth Reorientation in Arabidopsis Trichomes. *Plant Cell* **2000**, *12*, 465−477.
(14) Glas, J. J.; Schimmel, B. C. J.; Alba, J. M.; Escobar-Bravo, R.; Schuurink, R. C.; Kant, M. R. Plant Glandular Trichomes as Targets for Breeding or Engineering of Resistance to Herbivores. *Int. J. Mol. Sci.* **2012**, *13*, 17077−17103.
(15) Bjorkman, C.; Dalin, P.; Ahrne, K. Leaf Trichome Responses to Herbivory in Willows: Induction, Relaxation and Costs. *New Phytol.* **2008**, *179*, 176−184.
(16) Schellmann, S.; Hulskamp, M. Epidermal Differentiation: Trichomes in Arabidopsis as a Model System. *Int. J. Dev. Biol.* **2005**, *49*, 579−584.
(17) Schwab, B.; Folkers, U.; Ilgenfritz, H.; Hulskamp, M. Trichome Morphogenesis in Arabidopsis. *Philos. Trans. R. Soc., B* **2000**, *355*, 879−883.
(18) Yu, N.; Cai, W. J.; Wang, S. C.; Shan, C. M.; Wang, L. J.; Chen, X. Y. Temporal Control of Trichome Distribution by Microrna156-Targeted Spl Genes in Arabidopsis Thaliana. *Plant Cell* **2010**, *22*, 2322−2335.
(19) Sato, Y.; Kudoh, H. Tests of Associational Defence Provided by Hairy Plants for Glabrous Plants of Arabidopsis Halleri Subsp Gemmifera against Insect Herbivores. *Ecol. Entomol.* **2015**, *40*, 269−279.
(20) Clauss, M. J.; Dietel, S.; Schubert, G.; Mitchell-Olds, T. Glucosinolate and Trichome Defenses in a Natural Arabidopsis Lyrata Population. *J. Chem. Ecol.* **2006**, *32*, 2351−2373.
(21) Monshausen, G. B.; Gilroy, S. Feeling Green: Mechanosensing in Plants. *Trends Cell Biol.* **2009**, *19*, 228−235.
(22) Puentes, A.; Agren, J. Trichome Production and Variation in Young Plant Resistance to the Specialist Insect Herbivore Plutella Xylostella among Natural Populations of Arabidopsis Lyrata. *Entomol. Exp. Appl.* **2013**, *149*, 166−176.
(23) Zhou, L. H.; Liu, S. B.; Wang, P. F.; Lu, T. J.; Xu, F.; Genin, G. M.; Pickard, B. G. The Arabidopsis Trichome Is an Active Mechanosensory Switch. *Plant, Cell Environ.* **2016**, DOI: 10.1111/pce.12728.
(24) Zajaczkowska, U.; Kucharski, S.; Guzek, D. Are Trichomes Involved in the Biomechanical Systems of Cucurbita Leaf Petioles? *Planta* **2015**, *242*, 1453.
(25) Zust, T.; Joseph, B.; Shimizu, K. K.; Kliebenstein, D. J.; Turnbull, L. A. Using Knockout Mutants to Reveal the Growth Costs of Defensive Traits. *Proc. R. Soc. London, Ser. B* **2011**, *278*, 2598−2603.
(26) Paul-Victor, C.; Zust, T.; Rees, M.; Kliebenstein, D. J.; Turnbull, L. A. A New Method for Measuring Relative Growth Rate Can Uncover the Costs of Defensive Compounds in Arabidopsis Thaliana. *New Phytol.* **2010**, *187*, 1102−1111.
(27) Kliebenstein, D. J. Secondary Metabolites and Plant/Environment Interactions: A View through Arabidopsis Thaliana Tinged Glasses. *Plant, Cell Environ.* **2004**, *27*, 675−684.
(28) Ravilious, G. E.; Jez, J. M. Structural Biology of Plant Sulfur Metabolism: From Assimilation to Biosynthesis. *Nat. Prod. Rep.* **2012**, *29*, 1138−1152.
(29) Kulich, I.; Vojtikova, Z.; Glanc, M.; Ortmannova, J.; Rasmann, S.; Zarsky, V. Cell Wall Maturation of Arabidopsis Trichomes Is Dependent on Exocyst Subunit Exo70h4 and Involves Callose Deposition. *Plant Physiol.* **2015**, *168*, 120−U814.
(30) Wang, X. Q.; Ren, H. Q.; Zhang, B.; Fei, B. H.; Burgert, I. Cell Wall Structure and Formation of Maturing Fibres of Moso Bamboo (Phyllostachys Pubescens) Increase Buckling Resistance. *J. R. Soc., Interface* **2012**, *9*, 988−996.
(31) Marks, M. D.; Betancur, L.; Gilding, E.; Chen, F.; Bauer, S.; Wenger, J. P.; Dixon, R. A.; Haigler, C. H. A New Method for Isolating Large Quantities of Arabidopsis Trichomes for Transcriptome, Cell Wall and Other Types of Analyses. *Plant J.* **2008**, *56*, 483−492.
(32) He, J. W.; Cheng, L.; Gu, Z. B. A.; Hong, Y.; Li, Z. F. Effects of Low-Temperature Blanching on Tissue Firmness and Cell Wall Strengthening During Sweet Potato Flour Processing. *Int. J. Food Sci. Technol.* **2014**, *49*, 1360−1366.
(33) Demarty, M.; Morvan, C.; Thellier, M. Calcium and the Cell-Wall. *Plant, Cell Environ.* **1984**, *7*, 441−448.
(34) Alkeev, N.; Averin, S.; von Gratowski, S. New Method for Monitoring the Process of Freeze Drying of Biological Materials. *AAPS PharmSciTech* **2015**, *16*, 1474−1479.
(35) Kaneko, Y.; Matsushima, H.; Sekine, M.; Matsumoto, K. Preparation of Plant-Protoplasts for Sem Observation by Tert-Butanol Freeze-Drying Method. *J. Electron Microsc.* **1990**, *39*, 426−428.
(36) Lee, J. T. Y.; Chow, K. L. Sem Sample Preparation for Cells on 3d Scaffolds by Freeze-Drying and Hmds. *Scanning* **2012**, *34*, 12−25.
(37) Esch, J. J.; Chen, M.; Sanders, M.; Hillestad, M.; Ndkium, S.; Idelkope, B.; Neizer, J.; Marks, M. D. A Contradictory Glabra3 Allele Helps Define Gene Interactions Controlling Trichome Development in Arabidopsis. *Development* **2003**, *130*, 5885−5894.
(38) Hulskamp, M.; Misera, S.; Jurgens, G. Genetic Dissection of Trichome Cell-Development in Arabidopsis. *Cell* **1994**, *76*, 555−566.
(39) Marks, M. D.; Wenger, J. P.; Gilding, E.; Jilk, R.; Dixon, R. A. Transcriptome Analysis of Arabidopsis Wild-Type and Gl3-Sst Sim Trichomes Identifies Four Additional Genes Required for Trichome Development. *Mol. Plant* **2009**, *2*, 803−822.
(40) Goodspeed, D.; Chehab, E. W.; Min-Venditti, A.; Braam, J.; Covington, M. F. Arabidopsis Synchronizes Jasmonate-Mediated Defense with Insect Circadian Behavior. *Proc. Natl. Acad. Sci. U. S. A.* **2012**, *109*, 4674−4677.
(41) Voigt, D.; Gorb, S. Locomotion in a Sticky Terrain. *Arthropod-Plant Interactions* **2010**, *4*, 69−79.
(42) Brown, V. K.; Llewellyn, M. Variation in Aphid Weight and Reproductive Potential in Relation to Plant-Growth Form. *J. Anim. Ecol.* **1985**, *54*, 651−661.
(43) Kettles, G. J.; Drurey, C.; Schoonbeek, H. J.; Maule, A. J.; Hogenhout, S. A. Resistance of Arabidopsis Thaliana to the Green

DOI: 10.1021/acsami.6b02253
ACS Appl. Mater. Interfaces 2016, 8, 9755−9761

Peach Aphid, Myzus Persicae, Involves Camalexin and Is Regulated by Micrornas. *New Phytol.* **2013**, *198*, 1178−1190.

DOI: 10.1021/acsami.6b02253
ACS Appl. Mater. Interfaces 2016, 8, 9755−9761